Density Functional Theory Predictions of Second-Order Hyperpolarizabilities of Metallocenes

Nobuyuki Matsuzawa* and Jun'etsu Seto

SONY Corporation Research Center, 174 Fujitsuka-cho, Hodogaya-ku, Yokohama 240, Japan

David A. Dixon*,†

DuPont Central Research and Development, Experimental Station, P.O. Box 80328, Wilmington, Delaware 19880-0328‡

Received: August 23, 1995⊗

The geometries in the staggered and eclipsed conformations of the metallocenes, $M(C_5H_5)_2$ with M = Mn, Fe, Co, Ni, and Ru, have been calculated at the local and nonlocal density functional theory (LDFT and NLDFT) levels. The M−C distance is predicted to be too short at the LDFT level and too long at the NLDFT level. The doublet low-spin states for M = Mn and Co show distortions away from the idealized fivefold symmetries. The low-spin state for M = Mn is predicted to be lower in energy than the high-spin state in contrast to the observed experimental results. The size of the splitting is strongly dependent on the computational level. The values of α and γ were calculated for the various metallocenes. The highest value of γ was found for M = Co.

Introduction

There is significant interest in the development of nonlinear optical (NLO) materials because of their potential applications in electronic and optical devices. The NLO properties of organic materials have been extensively studied because of the ease of synthesis of such materials and the potential ease of processability.[1] Many of these materials have extended π electron systems, as this seems to be the easiest way to introduce large nonlinearities into organic systems.[1]

Nonlinearities for molecular systems can be expressed in terms of the hyperpolarizabilities defined in eq 1

$$\mu_i = \mu_i^\circ + \sum_j \alpha_{ij}F_j + \sum_{j,k} \beta_{ijk}F_jF_k/2 + \sum_{j,k,l} \gamma_{ijk}F_jF_kF_l/6 + ... \quad (1)$$

where μ_i is the dipole moment of a molecule under an applied field of F, μ_i° is the dipole moment without the applied field, α_{ij} is the polarizability, β_{ijk} is the hyperpolarizability, and γ_{ijkl} is the second-order hyperpolarizability. The subscripts i, j, k, and l denote Cartesian axes.

Because of the success of inorganic nonlinear optical materials such as $KTiOPO_4$ and $LiNbO_3$ for applications where the first-order hyperpolarizability is important, interest in organic nonlinear optical materials has focused more recently on the second-order hyperpolarizability (γ) for actual device applications. We have been using computational methods to predict the nonlinear optical behavior of a variety of molecules.[2,3] Although one can use semiempirical molecular orbital methods[4,5] for organic molecules in either finite field[2,4] or sum of states[5] approaches to predict β and γ, only the sum of states approach can be used for molecules containing transition metals, as there are few semiempirical molecular orbital parameters for transition metal systems outside of those implemented for spectroscopy predictions in computer programs such as ZINDO.[6] The sum of states approach is probably limited to studies of β as compared to γ because of slow convergence of the sum for the latter. Thus, one must rely on other methods to predict γ for molecules which contain transition metals. Although traditional ab initio molecular orbital methods can be used to provide benchmark studies for nonmetallic systems,[7] molecular orbital methods based on a single configuration often have difficulties in treating the electronic structure of molecules containing transition metals.[8] Furthermore, ab initio molecular orbital methods scale at least as N^5, where N is the number of molecular orbitals if correlation corrections are included and thus become computationally intractable for large systems. Density functional theory[9] (DFT) has proven to be an extremely useful tool for modeling transition metal systems, as its computational effort shows much better scaling with increasing molecular size (order N^3) and molecules with transition metals can be treated with a reasonable degree of accuracy.[10] We have previously reported DFT calculations on nonlinear optical properties of a number of systems including metalloporphines.[3] In order to further investigate the ability of DFT to predict the NLO properties of molecules containing transition metals, we describe below the results of DFT calculations on metallocenes. This allows us to further test the impact of the metal on the organic π electron system in a different type of geometry than found in the metalloporphines which we have previously studied.[3e]

There has been one previously reported calculation[11] of the value of γ for ferrocene at the CNDO level. Extended basis sets were used in a coupled Hartree−Fock approach. The calculated value (CHF-PT-EB-CNDO level) of 24.58×10^{-36} esu is significantly less than the experimental[12] value of $(96.2 \pm 10.8) \times 10^{-36}$ esu.

Calculations

The DFT calculations described below were done with the program system DMol[13] both at the local (LDFT) and nonlocal levels (NLDFT). The calculations have been described in detail previously.[3] The form for the exchange-correlation energy of

† Current address: Pacific Northwest National Laboratory, Environmental Molecular Sciences Laboratory, P.O. Box 999, MSK1-83, Richland, WA 99352.

‡ Contribution No. 7183.

⊗ Abstract published in *Advance ACS Abstracts,* January 1, 1996.

S1089-5639(95)02465-0 CCC: $14.00

the uniform electron gas for the LDFT calculations is that derived by von Barth and Hedin (BH).[13c] The NLDFT calculations were done with the gradient-corrected exchange potential of Becke[14] and the gradient-corrected correlation potential of Lee, Yang, and Parr (BLYP).[15] The calculations were done with a double numerical basis set augmented by polarization functions (DNP) and with a basis set (DNP+) obtained by augmenting the DNP basis set with the field-induced polarization (FIP) basis functions for C (spd) and H (p) given by Guan et al.[16] The spin-unrestricted open-shell formalism was used for open-shell molecules and a spin-restricted formalism was used for closed-shell molecules. Geometries were optimized by using analytic gradient methods with the DNP basis set.[13b] The density was converged to 10^{-6} for the geometry optimizations, and the FINE mesh was used.

The calculations of the nonlinear optical properties were done at the LDFT and NLDFT levels, except for the doublet state of manganocene, where we had significant convergence problems at the local level. A finite field approach[1] was used with the XFINE grid and the DNP and DNP+ basis sets; the density was converged to 10^{-8}. In this approach, the response of the ground state charge distribution to an external electric field at zero frequency is investigated. A molecule in an applied electric field will exhibit an induced dipole moment. This induced moment can be expanded in a Taylor series in powers of the electric field as shown in eq 1. The equations given by Sim et al.[17] for obtaining α, β, and γ from dipole moments calculated in an applied electric field (field strength[3] = 0.005 au unless otherwise noted) were used. The scalar values for α, β, and γ calculated from their vector or tensor components are defined as follows:

$$\alpha = \sum_i \alpha_{ii}/3 \tag{2}$$

$$\beta = (3/5)\sum_i \beta_i \mu_k / ||\mu|| \tag{3}$$

$$\gamma = \sum_{i,j} \gamma_{iijj}/5 \tag{4}$$

where $||\mu||$ and β_i are given as

$$\mu = ||\mu|| \tag{5}$$

$$\beta_i = \sum_j \beta_{ijj} \tag{6}$$

Results and Discussions

Calculations were done on the following metallocenes: magnanocene, ferrocene, cobaltocene, nickelocene, and ruthenocene. The numbering system of the atoms and the orientation of the molecule along the Cartesian axes are shown in Figure 1. For the metallocenes, the HOMO and LUMO consist predominantly of metal d orbitals (see discussion below), in contrast to the case of the metalloporphines previously studied,[3e] where the HOMO and LUMO are predominantly composed of π orbitals in the organic fragment. The order of the metal d orbitals in metallocenes in terms of energy is e_{2g} (d_{xy}, $d_{x^2-y^2}$) $\sim$ a_{1g} (d_{z^2}) < e_{1g} (d_{xz}, d_{yz}).[18] The electron configuration at the metal for ferrocene and ruthenocene is thus $(e_{2g})^4(a_{1g})^2$ if we make the usual assumption that the metal is in the M^{2+} charge state, so the ground state of ferrocene and ruthenocene should be a closed-shell singlet. For cobaltocene the configuration is $(e_{2g})^4(a_{1g})^2(e_{2g})^1$, and the resulting ground state should be a doublet. For nickelocene the electron configuration is $(e_{2g})^4(a_{1g})^2(e_{2g})^2$ and the ground state is a triplet.

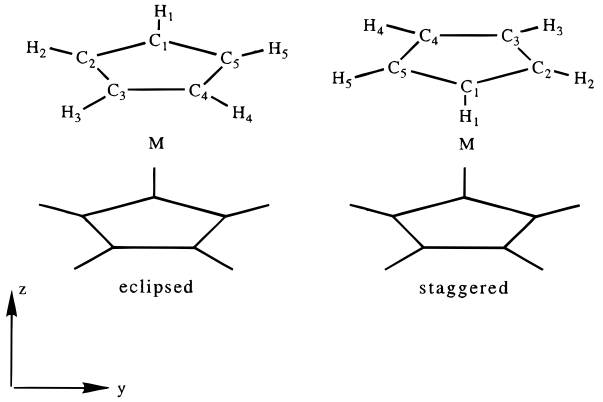

Figure 1. Numbering system of the atoms and the orientation along the Cartesian axes for the metallocene.

The description of the electronic structure of magnanocene, which has 5 d electrons for Mn^{2+}, is more complicated. A simple orbital-filling model yields configurations which are either $(e_{2g})^4(a_{1g})^1$ or $(e_{2g})^3(a_{1g})^2$, and the lowest energy doublet state is thought to be $^2E_{2g}$, which obviously will undergo a Jahn−Teller distortion. However, it is possible that the ligand field splitting is small enough so that all of the electrons are in separate orbitals, yielding a sextet state, $^6A_{1g}$. Both states were considered for manganocene. Besides the complexities introduced by the metal orbital occupancies, there are two possible conformers, staggered (D_{5d}) and eclipsed (D_{5h}), for the metallocenes, and both geometries were considered in the structural part of this study.

Geometries, Energies, and Orbital Levels. The LDFT (BH/DNP) optimized geometry parameters are shown in Table 1 together with experimental geometry parameters obtained from gas-phase electron diffraction measurements.[19] For the low-spin state of manganocene, we also include crystal structure results for decamethylmanganocene, which is of low spin.[20] The calculation predicted structures of D_{5d} or D_{5h} symmetry, except for the two doublet structures. The two doublet structures exhibit Jahn−Teller distortions away from the idealized D_{5d} or D_{5h} symmetry. The cyclopentadienyl (Cp) rings in cobaltocene and the doublet low-spin state of manganocene are no longer planar, yielding structures of C_{2h} and C_{2v} symmetry for the staggered and eclipsed conformers, respectively. This result for cobaltocene differs from the gas-phase electron diffraction results measured at ~120 °C, where it was suggested that any distortion from D_{5d} or D_{5h} symmetry is small.[19c] However, the electron diffraction measurements probably cannot distinguish the difference in symmetry at this temperature, as the rings are rapidly rotating about the approximate fivefold axis to give a structure with nominal fivefold symmetry. This is consistent with another experimental study of cobaltocene which reported unusually large Co−C vibrational amplitudes in the gas-phase structure consistent with the above discussion.[21] Furthermore, the crystal structure of decamethylmanganocene, which is low-spin, shows deviations from fivefold symmetry.[20]

The LDFT calculated geometry parameters for the eclipsed and staggered conformers do not differ significantly. The LDFT C−H bond lengths are shorter than the experimental values and fall within the experimental error limits, except for ruthenocene, manganocene (sextet), and nickelocene. For the former two metallocenes, the calculated values are shorter by ~0.03 Å than the experimental values, and we note that the experimental values are clearly too long. For nickelocene, the LDFT C−H bond lengths are longer than the experimental values, and the values approximately fall within the experimental error limits. The NLDFT C−H bond lengths are always shorter than the LDFT values by 0.005−0.007 Å.

TABLE 1: BH/DNP and BLYP/DNP Calculated Geometry Parameters[a]

	calc (eclipsed)		calc (staggered)		
	BH/DNP	BLYP/DNP	BH/DNP	BLYP/DNP	expt
			Manganocene(Doublet)[b]		
r(C−H)	1.094,[f] 1.094,[g] 1.095[h]	1.089,[f] 1.089,[g] 1.089[h]	1.096,[f] 1.096,[g] 1.096[h]	1.089,[f] 1.089,[g] 1.089[h]	
r(C−C)	1.430,[i] 1.420,[j] 1.412[k]	1.446,[i] 1.433,[j] 1.424[k]	1.431,[i] 1.420,[j] 1.413[k]	1.444,[i] 1.433,[j] 1.424[k]	1.418
d(C−Mn)	2.043,[l] 2.082,[m] 2.148[n]	2.117,[l] 2.157,[m] 2.233[n]	2.049,[l] 2.080,[m] 2.135[n]	2.129,[l] 2.163,[m] 2.231[n]	2.112 (2.144) *2.130*
d(Cp−Cp)	3.233,[o] 3.371,[p] 3.599[q]	3.415,[o] 3.540,[p] 3.777[q]	3.423[u]	3.610[u]	
τ(H−C−C−C)	−176.3,[r] −178.1,[s] 179.2[t]	−177.3,[r] 180.0,[s] 177.6[t]	175.3,[r] 177.6,[s] 180.0[t]	177.5,[r] 180.0,[s] −177.4[t]	
			Manganocene(Sextet)[b]		
r(C−H)	1.095	1.090	1.095	1.090	1.125 ± 0.010
r(C−C)	1.418	1.432	1.418	1.432	1.429 ± 0.008
d(C−Mn)	2.337	2.474	2.338	2.474	2.380 ± 0.006 (2.433)
d(Cp−Cp)	4.004	4.306	4.004	4.307	
τ(H−C−C−C)	180.0	−179.0	180.0	−179.1	
			Ferrocene[c]		
r(C−H)	1.094	1.088	1.094	1.088	1.104 ± 0.006
r(C−C)	1.428	1.439	1.426	1.439	1.440 ± 0.002
d(C−Fe)	2.013	2.097	2.017	2.101	2.064 ± 0.003
d(Cp−Cp)	3.211	3.406	3.222	3.405	
τ(H−C−C−C)	177.7	178.9	177.1	178.7	
			Cobaltocene[d]		
r(C−H)	1.095,[f] 1.093,[g] 1.094[h]	1.089,[f] 1.088,[g] 1.088[h]	1.095,[f] 1.093,[g] 1.094[h]	1.089,[f] 1.088,[g] 1.088[h]	1.095 ± 0.008
r(C−C)	1.430,[i] 1.411,[j] 1.441[k]	1.443,[i] 1.423,[j] 1.453[k]	1.430,[i] 1.410,[k] 1.441[k]	1.443,[i] 1.423,[j] 1.453[k]	1.430 ± 0.0015
d(C−Co)	2.034,[l] 2.100,[m] 2.052[n]	2.127,[l] 2.184,[m] 2.149[n]	2.039,[l] 2.105,[m] 2.060[n]	2.130,[l] 2.185,[m] 2.151[n]	2.113 ± 0.0015
d(Cp−Cp)	3.278,[o] 3.414,[p] 3.326[q]	3.493,[o] 3.607,[p] 3.545[q]	3.367[u]	3.564[u]	
τ(H−C−C−C)	177.0,[r] 177.2,[s] 180.0[t]	178.3,[r] 178.6,[s] 180.0[t]	177.1,[r] 178.1,[s] 180.0[t]	178.4,[r] 178.3,[s] 180.0[t]	176.40 ± 1.66
			Nickelocene[e]		
r(C−H)	1.094	1.089	1.094	1.089	1.083 ± 0.0095
r(C−C)	1.421	1.434	1.422	1.434	1.430 ± 0.0015
d(C−Ni)	2.143	2.238	2.139	2.239	2.196 ± 0.004
d(Cp−Cp)	3.539	3.752	3.528	3.754	
τ(H−C−C−C)	178.3	180.0	178.0	180.0	179.72 ± 1.45
			Ruthenocene[c]		
r(C−H)	1.094	1.088	1.094	1.088	1.130 ± 0.006
r(C−C)	1.428	1.440	1.428	1.440	1.439 ± 0.002
d(C−Ru)	2.185	2.267	2.185	2.268	2.196 ± 0.003
d(Cp−Cp)	3.631	3.815	3.631	3.818	
τ(H−C−C−C)	179.8	180.0	179.3	180.0	

[a] Distances in Å, angles in degrees. d(Cp−Cp) is the distance between the two pentagons consisting of five carbon atoms. [b] Experimental values for low-spin manganocene from ref 20 obtained from the X-ray crystal structure of decamethylmanganocene. Experimental values for high-spin manganocene from ref 19a in the gas-phase. Value in parentheses is for gas-phase 1,1′-dimethylmanganocene from ref 19e, and the italicized value is for gas-phase decamethylmanganocene from ref 19f. [c] Experimental values from ref 19b. [d] Experimental values from ref 19c. [e] Experimental values from ref 19d. [f] $r(C_1-H_1)$. [g] $r(C_2-H_2) = r(C_5-H_5)$. [h] $r(C_3-H_3) = r(C_4-H_4)$. [i] $r(C_1-C_2) = r(C_1-C_5)$. [j] $r(C_2-C_3) = r(C_4-C_5)$. [k] $r(C_3-C_4)$. [l] $r(M-C_1)$. [m] $r(M-C_2) = r(M-C_5)$. [n] $r(M-C_3) = r(M-C_4)$. [o] $r(C_1-C_1')$. [p] $r(C_2-C_2') = r(C_5-C_5')$. [q] $r(C_3-C_3') = r(C_4-C_4')$. [r] $\tau(H_1-C_1-C_5-C_4)$. [s] $\tau(H_5-C_5-C_4-C_3)$. [t] $\tau(H_4-C_4-C_3-C_2)$. [u] Averaged value.

Reasonable agreement for the C−C bond lengths was found for the manganocene doublet (averaged values of 1.423 and 1.422 Å for the staggered and eclipsed conformers, respectively, at the LDFT level), cobaltocene (averaged values of 1.424 and 1.425 Å for the staggered and eclipsed conformers, respectively, at the LDFT level), and nickelocene with differences between theory and experiment less than 0.008 Å at the LDFT level. For manganocene (sextet), ferrocene, and ruthenocene, the agreement at the LDFT level is still reasonable with the calculated values shorter than the experimental values by 0.011−0.014 Å. If nonlocal corrections are included, the C−C bond lengths are longer than the LDFT values, and the differences between the theoretical and experimental values are now less than 0.004 Å expect for the doublets. For the doublets, the agreement between theory and experiment becomes worse when nonlocal corrections are included, with the calculated values longer by 0.007−0.018 Å as compared to experiment.

A larger disagreement was found for the metal−carbon distances. Consistent with previous LDFT calculations, the LDFT calculated values are shorter than the experimental values by ∼0.01 Å,[22] ∼0.04 Å, ∼0.05 Å, ∼0.04 Å,[22] ∼0.04 Å, and ∼0.01 Å for manganocene (doublet), manganocene (sextet), ferrocene, cobaltocene, nickelocene, and ruthenocene, respectively. The τ(H−C−C−C) torsion angles calculated at the LDFT and NLDFT levels are in agreement with the experimental values, although the experimental error is quite large and all of the experimental values are not available. The LDFT and NLDFT calculations predict the Cp hydrogen atoms to be located closer to the metal atom as compared to the carbons in agreement with experimental studies[19,23] except for ruthenocene and doublet manganocene at the NLDFT level. For doublet manganocene, the Cp rings are not planar because of the Jahn−Teller distortion.

The inclusion of nonlocal corrections can lead to an improvement in the prediction of the M−C distance, as shown by Bérces et al., who reported r(Fe−C) = 2.048 Å for ferrocene.[24] The inclusion of nonlocal corrections does little to change the geometries of the cyclopentadienyl rings but does significantly affect the M−C bond distances. For ferrocene, the NLDFT Fe−C distance (for the eclipsed conformer) is 0.033 Å too long whereas, for ruthenocene, the NLDFT Ru−C distance is now 0.071 Å too long, but this error could be in part due to the need for relativistic corrections for Ru which are not present in the calculations. For cobaltocene the Co−C distance is too long by 0.046 Å at the NLDFT level, and for nickelocene the Ni−C distance is 0.042 Å too long. For the $^6A_{1g}$ state of manganocene,

TABLE 2: BH/DNP and BLYP/DNP Calculated Relative Energies of the Spin States and Conformers of the Metallocenes ($C_5H_5MC_5H_5$) in kcal/mol

	relative energy of the spin states of manganocene			
	eclipsed		staggered	
	BH	BLYP	BH	BLYP
doublet	0.00	0.00	0.00	0.00
sextet	36.84	12.13	35.96	11.77

	relative energy of the conformers											
	M = Mn											
	doublet		sextet		M = Fe		M = Co		M = Ni		M = Ru	
	BH	BLYP	BH	BLYP	BH	BLYP	BH	BLYP	BH	BLYP	BH	BLYP
eclipsed[a]	0.00	0.00	0.00	0.00	0.00	0.00	0.00	0.00	0.00	0.00	0.00	0.00
staggered	0.84	0.34	−0.04	−0.01	1.05	0.53	0.49	0.18	0.13	0.01	0.42	0.21

[a] BH/DNP calculated energies of the eclipsed conformer are −1532.488 957, −1532.430 254, −1645.151 877, −1764.068 100, −1889.482 777, and −4822.899 381 au for manganocene(doublet), manganocene(sextet), ferrocene, cobaltocene, nickelocene, and ruthenocene, respectively. BLYP/DNP calculated energies of the eclipsed conformer are −1538.109 014, −1538.089 690, −1650.875 510, −1769.925 763, −1895.475 796, and −4830.922 119 au for manganocene(doublet), manganocene(sextet), ferrocene, cobaltocene, nickelocene, and ruthenocene, respectively.

TABLE 3: Relative Energies (kcal/mol) and Selected Geometry Parameters (Å) for Distorted and Undistorted Doublet States[a]

	manganocene (doublet)					
	relative energy (kcal/mol)		*r*(C−Mn) (Å)		*r*(C−C) (Å)	
	eclipsed BH	staggered BH	eclipsed BH	staggered BH	eclipsed BH	staggered BH
distorted	0.00	0.00	2.101	2.096	1.425	1.423
undistorted	0.71	0.44	2.072	2.075	1.422	1.425

	cobaltocene (doublet)											
	relative energy (kcal/mol)				*r*(C−Co) (Å)				*r*(C−C) (Å)			
	eclipsed		staggered		eclipsed		staggered		eclipsed		staggered	
	BH	BLYP	BH	BLYP	BH	BLYP	BH	BLYP	BH	BLYP	BH	BLYP
distorted	0.00	0.00	0.00	0.00	2.068	2.159	2.074	2.160	1.425	1.437	1.424	1.437
undistorted	1.18	0.97	1.11	0.98	2.071	2.163	2.075	2.166	1.424	1.436	1.423	1.436

[a] Distorted geometries obtained without smearing of the charge distribution. Undistorted geometries obtained by smearing of the charge distribution. See text.

the Mn−C distance is 0.094 Å too long at the NLDFT level. For the doublet state of manganocene, the Mn−C distance can be compared to that reported in the gas phase[19e] for 1,1′-dimethylmanganocene, 2.144(12) Å, or to that reported in the crystal[20] for decamethylmanganocene, 2.112 Å. The other reported Mn−C distance is 2.130 Å from the gas-phase electron diffraction measurement for decamethylmanganocene.[19f] The average calculated value of 2.179 Å for the eclipsed conformer is 0.035 or 0.049 Å longer than the gas-phase values[19e,f] and 0.067 Å longer than the crystal structure value.[20] The agreement with experiment in either case is better than found for the sextet state.

The energies of the staggered conformer relative to those of the eclipsed conformer are shown in Table 2. The calculations predict that the eclipsed conformer is more stable than the staggered conformer with the difference in energies being quite small, $< \sim 1$ kcal/mol. The only exception is for the sextet state of manganocene, where the staggered structure is of essentially the same energy as the eclipsed one. This is not surprising, as the M−C distance is almost 0.3 Å longer than in the other metallocenes with first-row transition metals and the steric interactions between the rings should be smaller. In all cases the difference in energies is smaller at the NLDFT level as compared to the LDFT level consistent with the longer M−C distances predicted at the NLDFT level which separate the rings by a larger amount leading to reduced steric effects. The experimental result for ferrocene showed that the equilibrium conformation is eclipsed,[19b] consistent with our result. It was also reported that the barrier to the internal rotation of ferrocene is 0.9 ± 0.3 kcal/mol,[19b] in excellent agreement with our calculated values and with the nonlocal DFT value of 0.69 kcal/mol previously reported.[24] It has been suggested[19b] that the equilibrium conformation of ruthenocene is eclipsed, consistent with the DFT results. Hedberg et al. reported that their gas-phase electron diffraction result for cobaltocene is consistent with a free-rotation model for the Cp rings and suggested that the rotational barrier height would be in the order ferrocene > cobaltocene > nickelocene.[19c] The calculations are consistent with this, and for the latter two, essentially free rotation is predicted at the NLDFT level.

The electronic ground states of manganocenes are either high spin or low spin depending on the substituent.[25] The parent manganocene has been shown to be high spin by a variety of measurements. However, the calculations predict the low spin state to be of lower energy. The energy difference between the two states is predicted to be more than 30 kcal/mol at the local level. This difference is improved by including nonlocal corrections to give a value of 12.1 kcal/mol for the staggered geometry.

If integer occupation numbers are used, the doublet states of manganocene and cobaltocene exhibit a Jahn−Teller distortion. We reoptimized these structures with the electrons smeared at the Fermi level, i.e., noninteger occupation numbers, so that a symmetric structure could be examined. The BH/DNP and BLYP/DNP energies and selected geometry parameters are shown in Table 3. The optimized geometries at the LDFT and NLDFT levels for the doublets with the smeared charge distribution do not exhibit Jahn−Teller distortions, having D_{5h} and D_{5d} symmetry for the eclipsed and staggered conformers, respectively, as expected. For cobaltocene, the HOMO consists

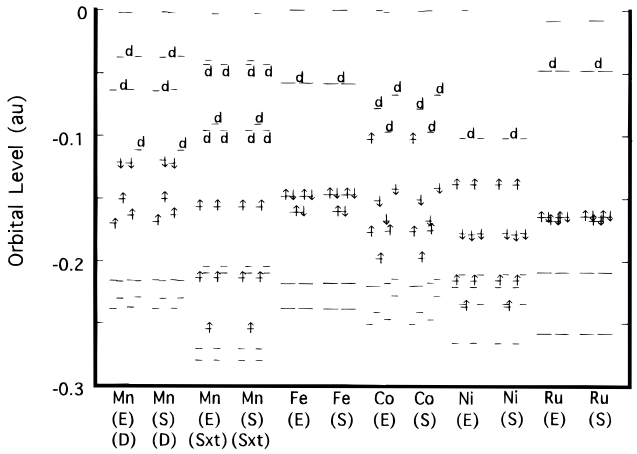

Figure 2. BLYP/DNP calculated energy levels of the metallocenes. Levels with marks of ↑, ↓, ↑↓, and d correspond to d orbitals, with the first three marks (↑, ↓, and ↑↓) showing the occupation of d-orbitals. E = eclipsed. S = staggered. D = doublet. Sxt = sextet.

of a degenerate e_{2g} orbital occupied by one electron. If smearing is not applied, one of the degenerate orbitals is singly occupied whereas, if the charge distribution is smeared, fractional occupation occurs with half of an electron in each of the two e_{2g} orbitals. A similar situation is found for manganocene with the configuration $(e_{2g})^3(a_{1g})^2$. The e_{2g} orbitals split apart with one electron in one orbital and two in the other if smearing is not used. If smearing is used, approximately 1.7 electrons are placed in each of the a_{1g} and e_{2g} orbitals, giving a symmetric structure. The energies of the symmetric (smeared) structures are higher than those of the distorted structures (no smearing). The energy difference between the symmetric and asymmetric structures gives the energy needed to reach the conical intersection, and it is very low, less than 0.75 kcal/mol for manganocene and less than 1.25 kcal/mol for cobaltocene. These results are consistent the observation in an electron diffraction experiment of an averaged structure with D_{5d} symmetry for cobaltocene. The calculated average structural parameters with or without smearing are essentially the same for cobaltocene, whereas, for manganocene, the metal carbon lengths calculated with smearing are shorter by 0.02−0.03 Å than those without smearing.

The molecular orbital energies at the BLYP/DNP level for the metallocenes are shown in Figure 2. The orbitals are essentially the same for the eclipsed and staggered conformers. The DFT calculations show that the HOMO for the metallocenes is localized on the metal. The order of the highest occupied d orbitals is a_{1g} (d_{z^2}) < e_{2g} (d_{xy}, $d_{x^2-y^2}$) < e_{1g} (d_{xz}, d_{yz}) except for the manganocene doublet, although we note that the difference in energy between the e_{2g} and a_{1g} levels is very small for ruthenocene. For the manganocene doublet, this ordering holds for the β-orbitals, whereas, for the α-orbitals, it is e_{2g} (d_{xy}, $d_{x^2-y^2}$) < a_{1g} (d_{z^2}) < e_{1g}(d_{xz}, d_{yz}). The order a_{1g} < e_{2g} < e_{1g} has previously been predicted for cobaltocene at the DFT level.[26] In contrast, ab initio molecular orbital calculations suggest that the highest occupied molecular orbitals reside on the Cp rings and that Koopmanns' theorem cannot be used.[27] If one performs SCF calculations on the ion, the orbital orderings then given are properly consistent with the experimental observations for ferrocene.[28]

The calculated charges and spin populations on the metal are shown in Table 4. The charge distributions are somewhat different between the local and nonlocal levels. The charges

TABLE 4: BH/DNP and BLYP/DNP Calculated Charges and Spin Densities of the Metallocenes[a]

	manganocene							
	doublet				sextet			
	eclipsed		staggered		eclipsed		staggered	
orbital	BH	BLYP	BH	BLYP	BH	BLYP	BH	BLYP
3d	5.97 (1.04)	5.91 (1.23)	5.98 (1.03)	5.92 (1.22)	5.57 (4.37)	5.46 (4.56)	5.57 (4.37)	5.46 (4.56)
d_{z^2}	1.78 (0.03)	1.79 (0.05)	1.78 (0.03)	1.80 (0.04)	1.01 (0.92)	1.01 (0.94)	1.01 (0.92)	1.01 (0.94)
d_{xy}, $d_{x^2-y^2}$	2.57 (0.91)	2.62 (0.99)	2.58 (0.90)	2.63 (0.99)	1.96 (1.93)	1.99 (1.97)	1.97 (1.93)	1.99 (1.97)
d_{xz}, d_{yz}	1.62 (0.10)	1.50 (0.19)	1.62 (0.10)	1.49 (0.19)	2.60 (1.52)	2.45 (1.65)	2.60 (1.52)	2.46 (1.65)
4s	0.49 (0.00)	0.44 (0.01)	0.49 (0.00)	0.45 (0.01)	0.40 (0.08)	0.32 (0.09)	0.40 (0.08)	0.32 (0.09)
4p	0.55 (0.03)	0.48 (0.04)	0.55 (0.03)	0.48 (0.04)	0.54 (0.10)	0.46 (0.12)	0.54 (0.10)	0.46 (0.12)
total on M	−0.03 (1.07)	0.15 (1.28)	−0.04 (1.06)	0.14 (1.27)	0.48 (4.54)	0.75 (4.77)	0.48 (4.54)	0.75 (4.77)

	ferrocene				cobaltocene			
	eclipsed		staggered		eclipsed		staggered	
orbital	BH	BLYP	BH	BLYP	BH	BLYP	BH	BLYP
3d	7.03	7.00	7.04	7.01	7.94 (0.67)	7.92 (0.80)	7.95 (0.68)	7.93 (0.80)
d_{z^2}	1.70	1.88	1.71	1.82	1.81 (0.01)	1.87 (0.03)	1.80 (0.03)	1.90 (0.02)
d_{xy}, $d_{x^2-y^2}$	3.45	3.37	3.47	3.43	3.62 (0.04)	3.65 (0.05)	3.65 (0.03)	3.63 (0.07)
d_{xz}, d_{yz}	1.89	1.75	1.87	1.74	2.50 (0.61)	2.40 (0.72)	2.50 (0.62)	2.40 (0.72)
4s	0.52	0.47	0.52	0.47	0.51 (0.00)	0.45 (−0.01)	0.51 (−0.01)	0.45 (−0.01)
4p	0.61	0.53	0.60	0.53	0.60 (0.01)	0.53 (0.01)	0.60 (0.01)	0.53 (0.01)
total on M	−0.15	−0.01	−0.17	−0.02	−0.07 (0.67)	0.09 (0.79)	−0.07 (0.67)	0.08 (0.79)

	nickelocene				ruthenocene			
	eclipsed		staggered		eclipsed		staggered	
orbital[b]	BH	BLYP	BH	BLYP	BH	BLYP	BH	BLYP
3d	8.80 (1.02)	8.80 (1.08)	8.80 (1.02)	8.80 (1.09)	6.98	7.06	7.00	7.07
d_{z^2}	1.90 (0.02)	1.94 (0.02)	1.90 (0.02)	1.91 (0.02)	1.70	1.84	1.70	1.84
d_{xy}, $d_{x^2-y^2}$	3.81 (0.03)	3.82 (0.03)	3.81 (0.03)	3.85 (0.04)	3.44	3.42	3.44	3.43
d_{xz}, d_{yz}	3.10 (0.97)	3.04 (0.98)	3.11 (0.97)	3.04 (1.03)	1.86	1.80	1.86	1.80
4s	0.49 (−0.02)	0.43 (−0.03)	0.50 (−0.01)	0.43 (−0.03)	0.47	0.46	0.47	0.46
4p	0.60 (0.00)	0.53 (−0.01)	0.60 (0.00)	0.53 (−0.01)	0.48	0.44	0.48	0.44
total on M	0.12 (1.00)	0.24 (1.04)	0.09 (1.00)	0.24 (1.04)	0.09	0.07	0.08	0.06

[a] Charges in units of electrons. Numbers in parentheses are spin densities. [b] For ruthenocene, 3d, 4s, and 4p should be read as 4d, 5s, and 5p, respectively.

TABLE 5: LDFT and NLDFT Calculated Scalar Values of Polarizability and First- and Second-Order Hyperpolarizability of the Eclipsed Conformer of the Metallocenes[a]

	α				β				γ			
	BH/DNP 0.005[b]	BH/DNP+ 0.0025[b]	BH/DNP+ 0.005[b]	BLYP/DNP+ 0.005[b]	BH/DNP 0.005[b]	BH/DNP+ 0.0025[b]	BH/DNP+ 0.005[b]	BLYP/DNP+ 0.005[b]	BH/DNP 0.005[b]	BH/DNP+ 0.0025[b]	BH/DNP+ 0.005[b]	BLYP/DNP+ 0.005[b]
manganocene(D)[c,d]				2.065				0.871				58.12
manganocene(S)[c,d]			2.042	2.108							52.99	44.58
ferrocene[e]	1.871		1.894	1.992					19.57		26.82	34.01
cobaltocene(C_{2v})[d,f]	1.946	2.002	1.999	2.087	0.129	0.318	0.519	0.316	38.52	96.80	130.76	95.77
cobaltocene(D_{5h})[d,g]				2.093								98.08
nickelocene[d]	1.988	2.039	2.038	2.149					24.50	52.83	61.39	49.07
ruthenocene[e]	2.028		2.052	2.158					18.61		26.54	37.67

[a] Units are $\times 10^{-23}$ cm^3 for α, $\times 10^{-30}$ esu for β, and $\times 10^{-36}$ esu for γ. BH/DNP and BH/DNP+ values calculated at the BH/DNP optimized geometry. BLYP/DNP+ values calculated at the BLYP/DNP+ optimized geometry. [b] Applied field strength in au. [c] D = doublet. S = sextet. [d] Calculated at the spin-unrestricted level. [e] Calculated at the spin-restricted level. [f] Calculated at the Jahn−Teller distorted geometry without smearing. [g] Calculated at the D_{5h} geometry with smearing.

on the metal at the nonlocal level are generally more positive (less negative) except for ruthenocene. This is consistent with less backbonding from the ligands due to the longer M−C distances at the NLDFT level. The difference between the two computational levels is about 0.15 e except for the high-spin state of manganocene, where a larger difference of 0.27 e is found. The charge distribution for Fe in ferrocene at the nonlocal level shows that there are 7 electrons in the d orbitals, 0.5 electrons in the 4s orbitals, and 0.5 electrons in the 4p orbitals. Overall, the charge on the Fe is essentially neutral. A similar charge distribution is found for ruthenocene except that there is less charge in the valence 5p orbital, about 0.1 e, so that the Ru is now slightly positive with charges of 0.06 e and 0.07 e for the two conformers at the NLDFT level. For cobaltocene, the additional electron goes predominantly into the d_{xz} and d_{yz} orbitals with the d_{z^2} orbitals gaining −0.01 e (eclipsed) and 0.08 e (staggered) and the d_{xy} and $d_{x^2-y^2}$ orbitals gaining 0.28 e (eclipsed) and 0.20 e (staggered) at the NLDFT level. The remainder of the charge distribution is like that in ferrocene, although the Co is somewhat less negative than the Fe with charges of 0.09 e and 0.08 e on the Co for the two conformers. As would be expected, most of the spin is on the metal, 0.80 e, with this spin residing in the d_{xz} and d_{yz} orbitals (0.72 e). According to the spin densities on Ni, nickelocene is a triplet with one spin on the metal and one spin localized on the rings. The changes in the electron distribution found in substituting Co for Fe are the same as those for substituting Ni for Co. For nickelocene, the Ni is actually positive with a charge of 0.24 e. Again the spin is localized in the d_{xz} and d_{yz} orbitals.

For sextet manganocene, there are an additional 0.5 electrons in the d_{xz} and d_{yz} orbitals over that predicted from a simple orbital-filling model. There are also 0.32 e in the valence 4s orbital and 0.46 e in the 4p orbitals, consistent with the results for the other metallocenes, although the value in the 4s orbital is somewhat smaller than those for the other compounds. There is a significant difference in the charge on the metal of almost 0.3 e at the local and nonlocal levels. Most of the spin resides on the metal with 0.46 e of spin on the ligand at the local level and 0.23 e on the ligand at the nonlocal level. The doublet state of manganocene is predicted to have a slightly positive metal at the NLDFT level in contrast to the much higher positive charge predicted for the sextet state. The orbital populations suggest that the d_{z^2} orbital is mostly occupied, but there are only 1.5 electrons in the d_{xz} and d_{yz} orbitals and 2.6 e in the d_{xy} and $d_{x^2-y^2}$ orbitals. All of the positive spin is on the metal in cobaltocene with a negative spin density on the ligands (−0.3 e). The spin is predicted to be mostly localized in the d_{xy} and $d_{x^2-y^2}$ in-plane orbitals.

Polarizabilities and First- and Second-Order Hyperpolarizabilities. The scalar values for the polarizabilities (α), first-order hyperpolarizabilities (β), and second-order hyperpolarizabilities (γ) at the BH/DNP, BH/DNP+, and BLYP/DNP+ levels for the metallocenes are shown in Table 5, and the tensor components are in Table 6. We calculated the values for the eclipsed conformer (D_{5h} or C_{2v}), as this conformer is usually more stable than the staggered conformer (D_{5d} or C_{2h}). Values of β are only given for doublet manganocene and cobaltocene, where a Jahn−Teller distortion is found, and for the others, the value of β is zero by symmetry.

For α, the predicted values do not strongly depend on the computational parameters, such as the applied finite field strength and basis sets, and are in the order ferrocene < manganocene(doublet) < cobaltocene < manganocene(sextet) < nickelocene < ruthenocene at the NLDFT level. The BH/DNP+ values are larger by 1−3% as compared to the BH/DNP values, as found in our previous study on substituted benzenes.[3b] The BH/DNP+ values at 0.0025 au are slightly larger than the BH/DNP+ values at 0.005 au, although the difference is less than 1%. These results clearly show that these values are well converged. The inclusion of nonlocal corrections increases the value of α by about 3−5%, comparable to the improvement due to adding diffuse functions to the basis set.[3] The calculated value of α for ferrocene of 1.99×10^{-23} cm^3 is in excellent agreement with the experimental value[29] of 1.90×10^{-23} cm^3. At the CHF-PT-EB-CNDO level,[11] the value of α is calculated to be slightly too high at 2.16×10^{-23} cm^3.

The values of β for doublet manganocene and cobaltocene are quite small. This is consistent with the small dipole moments and with the very low energies needed to reach the symmetric structure from the distorted structure. Thus, the doublets do not strongly deviate from the ideal D_{5d} symmetry and the value of β would be expected to be near zero. The various components of the β tensor are consistent with this result and are small. The scalar value of β for manganocene is larger than that for cobaltocene, consistent with the larger distortion from D_{5h} symmetry predicted for the former as compared to the latter, as discussed above. For example, the difference in the distances between the carbons in the two Cp rings can be as large as 0.366 Å for manganocene, whereas, for cobaltocene, it is only as large as 0.136 Å. The difference in the degree of the distortion could account for the difference in the calculated β values for these two species.

The BH/DNP+ value for γ at 0.005 au is larger by about 40% for ferrocene and ruthenocene as compared to the BH/DNP value at 0.005 au, consistent with our previous calculations on benzene derivatives.[3b] A significantly larger enhancement due to the addition of diffuse functions is predicted for

TABLE 6: LDFT and NLDFT Calculated Tensor Components Polarizability and Second-Order Hyperpolarizability of the Eclipsed Conformer of the Metallocenes[a]

	BH/DNP+	BLYP/DNP+		BH/DNP+	BLYP/DNP+		BH/DNP+	BLYP/DNP+
				Manganocene(Doublet)[b,d]				
μ_x		−0.34405	α_{xx}		1.8578	α_{yy}		1.8387
α_{zz}		2.4976	β_{xxx}		−0.693	β_{xyy}		−0.289
β_{xzz}		−0.469	β_x		−1.452	τ_{xxxx}		49.88
γ_{yyyy}		42.19	γ_{zzzz}		69.16	γ_{xxyy}		12.08
γ_{xxzz}		25.66	γ_{yyzz}		26.96			
				Manganocene(Sextet)[b]				
$\alpha_{xx} = \alpha_{yy}$	1.9387	1.9933	α_{zz}	2.2477	2.3387			
$\gamma_{xxxx} = \gamma_{yyyy}$	24.93	26.03	γ_{zzzz}	90.71	69.27	γ_{xxyy}	7.99	8.93
$\gamma_{xxzz} = \gamma_{yyzz}$	27.10	20.93						
				Ferrocene[c]				
$\alpha_{xx} = \alpha_{yy}$	1.7324	1.7778	α_{zz}	2.2164	2.4193			
$\gamma_{xxxx} = \gamma_{yyyy}$	24.16	27.51	γ_{zzzz}	27.27	39.67	γ_{xxyy}	7.57	8.41
$\gamma_{xxzz} = \gamma_{yyzz}$	10.84	14.64						
				Cobaltocene (C_{2v})[b,d]				
μ_x	−0.02637	−0.01697	α_{xx}	1.7708	1.8167	α_{yy}	1.8557	1.8764
α_{zz}	2.3717	2.5666	β_{xxx}	0.398	0.388	β_{xyy}	−0.851	−0.579
β_{xzz}	−0.412	−0.337	β_x	−0.865	−0.527	γ_{xxxx}	22.42	26.76
γ_{yyyy}	106.75	80.72	γ_{zzzz}	166.10	107.45	γ_{xxyy}	19.47	15.59
γ_{xxzz}	25.57	24.31	γ_{yyzz}	134.22	92.05			
				Nickelocene[b]				
$\alpha_{xx} = \alpha_{yy}$	1.8390	1.8780	α_{zz}	2.4370	2.6899			
$\gamma_{xxxx} = \gamma_{yyyy}$	31.60	29.50	γ_{zzzz}	87.20	68.45	γ_{xxyy}	9.82	8.12
$\gamma_{xxzz} = \gamma_{yyzz}$	34.23	25.42						
				Ruthenocene[c]				
$\alpha_{xx} = \alpha_{yy}$	1.7900	1.8368	α_{zz}	2.5756	2.7991			
$\gamma_{xxxx} = \gamma_{yyyy}$	17.27	24.36	γ_{zzzz}	40.26	56.63	γ_{xxyy}	5.58	11.32
$\gamma_{xxzz} = \gamma_{yyzz}$	11.69	15.09						

[a] Units are $\times 10^{-18}$ esu, $\times 10^{-23}$ cm^3, $\times 10^{-30}$ esu, and $\times 10^{-36}$ esu for μ, α, β, and γ, respectively. Only non-zero components are shown. Applied finite field strength = 0.005 au. BH/DNP and BH/DNP+ values calculated at the BH/DNP optimized geometry. BLYP/DNP+ values calculated at the BLYP/DNP+ optimized geometry. [b] Calculated at the spin-unrestricted level. [c] Calculated at the spin-restricted level. [d] Calculated at the Jahn−Teller distorted geometry with integral occupation numbers.

cobaltocene and nickelocene. The BH/DNP+ value is 3.4 and 2.5 times larger than the BH/DNP value for cobaltocene and nickelocene, respectively. We also calculated the BH/DNP+ value at a field strength of 0.0025 au for these two compounds, and this yielded values which are smaller by 14−26% than those at 0.005 au, exhibiting a somewhat larger dependence of γ on the applied field strength than usually observed.[3b] Inclusion of nonlocal corrections leads to different effects. For the closed-shell metallocenes, the value for ferrocene is raised by 27% whereas that for ruthenocene is raised by 42%. For the open-shell species, where a comparison can be made, the effect of nonlocal corrections is to lower the value of γ by about 20%.

The best calculated value for ferrocene at the DFT level of 34.01×10^{-36} esu is about a factor of 3 less than the experimental[12] value of $(96.2 \pm 10.8) \times 10^{-36}$ esu and is about 50% higher than the CHF-PT-EB-CNDO value[11] of 24.58×10^{-36} esu. Two possibilities exist for the discrepancy between the DFT value and experiment. The basis set for the DFT calculations may not be adequate enough, and the experimental value may not have been extrapolated back to zero frequency.

The calculated γ values at the BLYP/DNP+ level are in the order ferrocene ∼ ruthenocene < manganocene(sextet) < nickelocene < manganocene(doublet) < cobaltocene. The values of γ for all of the metallocenes fall in the range $(30-60) \times 10^{-36}$ esu except that for cobaltocene, which is almost 100×10^{-36} esu. The doublet states have the highest values for γ. We also calculated γ for doublet cobaltocene in D_{5h} symmetry at the BYLP/DNP optimized geometry. This geometry was obtained by smearing the electrons at the Fermi level, and the calculation of γ was obtained with this technique. This calculation yielded a value of 98.08×10^{-36} esu for γ, essentially the same as the value of 95.77×10^{-36} esu obtained for the distorted geometry where there are no fractional occupancies. This shows that the enhanced values of γ for the doublet species cannot be attributed to the distortion in geometry. This is consistent with the small values of β as discussed above. This suggests that the presence of an unpaired spin helps to increase the value of γ. We note that the HOMO levels of the doublets are predicted to have the highest values for the metallocenes that we studied (Figure 2).

Except for the doublets, the ordering of the magnitude of γ does not correlate with the ordering of the HOMO levels. For example, the HOMO of ferrocene is higher than that for ruthenocene, whereas the value of γ for ferrocene is smaller than that for ruthenocene. Furthermore, the order of the magnitude for γ does not correlate with the order of the calculated charges on the metal (Table 4), which are related to the degree of charge transfer between the metal and the Cp rings.

The quantity which does correlate with the magnitude of γ except for the doublets is the electron density in the d_{xz} and d_{yz} orbitals. The order of the charges is Ni (3.04) > Mn (sextet, 2.45) > Ru (1.80) > Fe (1.50), the same as the ordering of the magnitudes of γ. If the unpaired spin is placed in the d_{xz} or d_{yz} orbitals (e_{1g} molecular orbital), which are nominally antibonding, there is a larger increase in the magnitude of γ than found by placing the unpaired spin in the in-plane d_{xy} and $d_{x^2-y^2}$ orbitals or in the d_{z^2} orbital. The HOMO of the $(Cp)_2$ system should be an e_{1g} (or e_{1u}) orbital, whereas the LUMO is an e_{2g} (or e_{2u}) orbital. Thus the $d_{x^2-y^2}$, d_{xy}, and d_{z^2} orbitals (e_{2g} or a_{1g}) will not interact significantly with the HOMO of $(Cp)_2$ (e_{1g} or e_{1u}), and the charge distribution in the Cp rings in the ground state will be less impacted by changes in the electron population in these orbitals. The d_{xz} and d_{yz} orbitals (e_{1g}) can interact with the HOMO of $(Cp)_2$, and changes in the electron population in these orbitals can affect the charge distribution in the Cp rings, leading to changes in the value of γ.

Conclusions

The geometries in the staggered and eclipsed conformations of the metallocenes, $M(C_5H_5)_2$ with M = Mn, Fe, Co, Ni, and Ru, were calculated at the LDFT and NLDFT levels. The M−C distance is predicted to be too short at the LDFT level and too long at the NLDFT level. The doublet low-spin states for manganocene and cobaltocene show distortions away from the idealized fivefold symmetries. For manganocene, the doublet low-spin state is predicted to be lower than the sextet high-spin state in contrast to the observed experimental results. The size of the splitting in energy of the doublet and sextet manganocene is strongly dependent on the computational level, with NLDFT values being smaller than LDFT values but still too large as compared to experiment.

The values of α and γ were also calculated for the various metallocenes. The calculated values of α are essentially identical for the metallocenes, falling in the range $(1.99-2.16) \times 10^{-23}$ cm^3, whereas the values of γ differ significantly. The order of the calculated γ values is ferrocene < ruthenocene < manganocene(sextet) < nickelocene < manganocene(doublet) < cobaltocene, with the highest values found for the doublet species (95.77×10^{-36} esu and 58.12×10^{-36} esu for the cobaltocene and manganocene doublets, respectively). Except for the doublets, it is found that the magnitude of γ is affected by the electron density in the d_{xz} and d_{yz} orbitals (e_{1g} molecular orbital), which can interact with the HOMO of the $(Cp)_2$ system (e_{1g} or e_{1u} molecular orbital).

References and Notes

(1) For example: (a) *Nonlinear Optical Properties of Organic Molecules and Crystals*; Chemla, D. S., Zyss, J., Eds.; Academic Press: New York, 1987. (b) Williams, D. J. *Angew. Chem., Int. Ed. Engl.* **1994**, *23*, 690. (c) Marder, S. R.; Gorman, C. R.; Meyers, F.; Perry, J. W.; Bourhill, G.; Bredas, J.-L.; Pierce, B. M. *Science* **1994**, *265*, 632.

(2) (a) Matsuzawa, N.; Dixon, D. A. *J. Phys. Chem.* **1992**, *96*, 6232. (b) Matsuzawa, N.; Dixon, D. A. *Int. J. Quantum Chem.* **1992**, *44*, 497. (c) Matsuzawa, N.; Dixon, D. A. *J. Phys. Chem.* **1992**, *96*, 6241.

(3) (a) Matsuzawa, N.; Dixon, D. A. *J. Phys. Chem.* **1992**, *96*, 6872. (b) Matsuzawa, N.; Dixon, D. A. *J. Phys. Chem.* **1994**, *98*, 2545. (c) Dixon, D. A.; Matsuzawa, N. *J. Phys. Chem.* **1994**, *98*, 3967. (d) Matsuzawa, N.; Dixon, D. A. *J. Phys. Chem.* **1994**, *98*, 11677. (e) Matsuzawa, N.; Ata, M.; Dixon, D. A. *J. Phys. Chem.* **1995**, *99*, 7698.

(4) For example: (a) Dewar, M. J. S.; Yamaguchi, Y.; Suck, S. H. *Chem. Phys. Lett.* **1978**, *59*, 541. (b) Zyss, J. *J. Chem. Phys.* **1979**, *71*, 909. (c) Zyss, J. *J. Chem. Phys.* **1979**, *70*, 3341. (d) Williams, G. R. J. *J. Mol. Struct.* **1987**, *151*, 215. (e) Kurtz, H. A.; Stewart, J. J. P.; Dieter, K. M. *J. Comput. Chem.* **1990**, *11*, 82. (f) Waite, J.; Papadopoulos, M. G. *J. Phys. Chem.* **1991**, *95*, 5246. (g) Cardelino, B. H.; Moore, C. E.; Stickel, R. E. *J. Phys. Chem.* **1991**, *95*, 8645.

(5) For example: (a) Docherty, V. J.; Pugh, D.; Morley, J. O. *J. Chem. Soc., Faraday Trans. 2* **1985**, *81*, 1179. (b) Svendsen, E. N.; Willand, C. S.; Albrecht, A. C. *J. Chem. Phys.* **1985**, *83*, 5760. (c) Li, D.; Marks, T. J.; Ratner, M. A. *Chem. Phys. Lett.* **1986**, *131*, 370. (d) Morley, J. O.; Docherty, V. J.; Pugh, D. *J. Chem. Soc., Perkin Trans. 2* **1987**, 1351. (e) Morley, J. O.; Docherty, V. J.; Pugh, D. *J. Chem. Soc., Perkin Trans. 2* **1987**, 1357. (f) Morley, J. O.; Docherty, V. J.; Pugh, D. *J. Chem. Soc., Perkin Trans. 2* **1987**, 1361. (g) Morley, J. O. *J. Am. Chem. Soc.* **1988**, *110*, 7660. (h) Li, D.; Ratner, M. A.; Marks, T. J. *J. Am. Chem. Soc.* **1988**, *110*, 1707. (i) Pierce, B. M. *J. Chem. Phys.* **1989**, *91*, 791. (j) Parkinson, W. A.; Zerner, M. C. *J. Chem. Phys.* **1991**, *94*, 478. (k) Morley, J. O. *J. Chem. Soc., Faraday Trans.* **1991**, *87*, 3015. (l) Morley, J. O.; Pugh, D. *J. Chem. Soc., Faraday Trans.* **1991**, *87*, 3021. (m) Kanis, D. R.; Marks, T. J.; Ratner, M. A. *Int. J. Quantum Chem.* **1992**, *43*, 61. (n) Kanis, D. R.; Ratner, M. A.; Marks, T. J. *J. Am. Chem. Soc.* **1992**, *114*, 10338.

(6) (a) Zerner, M. C.; Loew, G. W.; Kirchner, R. F.; Mueller-Westerhoff, U. T. *J. Am. Chem. Soc.* **1980**, *102*, 589. (b) Anderson, W. P.; Cundari, T. R.; Drago, R. S.; Zerner, M. C. *Inorg. Chem.* **1990**, *29*, 1.

(7) For example: (a) McLean, A. D.; Yoshimine, M. *J. Chem. Phys.* **1967**, *46*, 3682. (b) Bartlett, R. J.; Purvis, D. D., III. *Phys. Rev. A* **1979**, *20*, 1313. (c) Huo, W. M.; Jaffe, R. L. *Phys. Rev. Lett.* **1981**, *47*, 30. (d) Jaszunski, M.; Roos, B. O. *Mol. Phys.* **1984**, *52*, 1209. (e) Dykstra, C. E. *J. Chem. Phys.* **1985**, *82*, 4120. (f) Sekino, H.; Bartlett, R. J. *J. Chem. Phys.* **1986**, *85*, 976. (g) Hurst, G. J. B.; Dupuis, M.; Clementi, E. *J. Phys. Chem.* **1988**, *89*, 385. (h) Karna, S. P.; Dupuis, M.; Perrin, E.; Prasad, P. N. *J. Chem. Phys.* **1990**, *92*, 7418. (i) Karna, S. P.; Dupuis, M. *Chem. Phys. Lett.* **1990**, *171*, 201. (j) Daniel, C.; Dupuis, M. *Chem. Phys. Lett.* **1990**, *171*, 209. (k) Karna, S. P.; Perrin, E.; Prasad, P. N.; Dupuis, M. *J. Phys. Chem.* **1991**, *95*, 4329. (l) Velders, G. J. M.; Gillet, J.-M.; Becker, P. J.; Feil, D. *J. Phys. Chem.* **1990**, *95*, 8601. (m) Rice, J. E.; Scuseria, G. E.; Lee, T. J.; Taylor, P. R.; Almlöf, J. *Chem. Phys. Lett.* **1992**, *191*, 23. (n) Kirtman, B.; Hasan, M. *J. Chem. Phys.* **1992**, *96*, 470. (o) Sim, F.; Chin, S.; Dupuis, M.; Rice, J. E. *J. Phys. Chem.* **1993**, *97*, 1158.

(8) For examples, see: (a) Lüthi, H. P.; Ammeter, J. H.; Almlöf, J.; Faegri, K., Jr. *J. Chem. Phys.* **1982**, *77*, 2002. (b) Lüthi, H. P.; Siegbahn, P. E. M.; Almlöf, J.; Faegri, K., Jr.; Hedberg, A. *Chem. Phys. Lett.* **1984**, *111*, 1. (c) Park, C.; Almlöf, J. *J. Chem. Phys.* **1991**, *95*, 1829.

(9) (a) Hohenberg, P.; Kohn, W. *Phys. Rev. B* **1964**, *136*, 864. (b) Kohn, W.; Sham, L. J. *Phys. Rev. A* **1965**, *140*, 1133. (c) Parr, R. G.; Yang, W. *Density Functional Theory of Atoms and Molecules*; Oxford University Press: New York, 1989. (d) Salahub, D. R. In *Ab Initio Methods in Quantum Chemistry—II*; Lawley, K. P., Ed.; John Wiley and Sons: New York, 1987; p 447. (e) Wimmer, E.; Freeman, A. J.; Fu, C.-L.; Cao, P.-L.; Chou, S.-H.; Delley, B. In *Supercomputer Research in Chemistry and Chemical Engineering*; Jensen, K. F., Truhlar, D. G., Eds.; ACS Symposium Series No. 353; American Chemical Society: Washington, D.C., 1987; p 49. (f) Jones, R. O.; Gunnarsson, O. *Rev. Mod. Phys.* **1989**, *61*, 689. (g) Ziegler, T. *Chem. Rev.* **1991**, *91*, 651. (h) Delley, B. In *Density Functional Theory in Chemistry*; Labanowski, J., Andzelm, J., Eds.; Springer-Verlag: New York, 1991; p 101.

(10) Sosa, C.; Andzelm, J.; Elkin, B. C.; Wimmer, E.; Dobbs, K. D.; Dixon, D. A. *J. Phys. Chem.* **1992**, *96*, 6630.

(11) Waite, J.; Papadopoulos, M. G. *J. Phys. Chem.* **1991**, *95*, 5426.

(12) Ghosal, S.; Samoc, M.; Prasad, P. N.; Tufariello, J. J. *J. Phys. Chem.* **1990**, *94*, 2847.

(13) (a) Delley, B. *J. Chem. Phys.* **1990**, *92*, 508. (b) Delley, B. *J. Chem. Phys.* **1991**, *94*, 7245. (c) von Barth, U.; Hedin, L. *J. Phys. C* **1972**, *5*, 1629. DMol is available commercially from MSI (BIOSYM Technologies), San Diego, CA.

(14) (a) Becke, A. D. *Phys. Rev. A* **1988**, *38*, 3098. (b) Becke, A. D. In *The Challenge of d and f Electrons: Theory and Computation*; Salahub, D. R., Zerner, M. C., Eds.; ACS Symposium Series No. 394; American Chemical Society: Washington, D.C., 1989; p 166. (c) Becke, A. D. *Int. J. Quantum Chem. Symp.* **1989**, *23*, 599.

(15) Lee, C.; Yang, W.; Parr, R. G. *Phys. Rev.* **1988**, *37*, 786.

(16) Guan, J.; Duffy, P.; Carter, J. T.; Chong, D. P.; Casida, K. C.; Casida, M. E.; Wrinn, M. *J. Chem. Phys.* **1993**, *98*, 4753.

(17) Sim, F.; Chin, S.; Dupuis, M.; Rice, J. E. *J. Phys. Chem.* **1993**, *97*, 1158.

(18) Yamamoto, A. *Chemistry of Organometallics*; Shokabo: Tokyo, 1982; p 67 (in Japanese).

(19) (a) Haaland, A. *Inorg. Nucl. Chem. Lett.* **1979**, *15*, 267. (b) Haaland, A.; Nilsson, J. E. *Acta Chem. Scand.* **1968**, *22*, 2653. (c) Hedberg, A. K.; Hedberg, L.; Hedberg, K. *J. Chem. Phys.* **1975**, *63*, 1262. (d) Hedberg, L.; Hedberg, K. *J. Chem. Phys.* **1970**, *53*, 1228. (e) Almenningen, A.; Haaland, A.; Samdal, S. *J. Organomet. Chem.* **1978**, *149*, 219. (f) Fernholt, L.; Haaland, A.; Seip, R.; Robbins, J. L.; Smart, J. C. *J. Organomet. Chem.* **1980**, *194*, 351.

(20) Freyberg, D. P.; Robbins, D. L.; Raymond, K. N.; Smart, J. C. *J. Am. Chem. Soc.* **1979**, *101*, 892.

(21) Almenningen, A.; Gard, E.; Haaland, A.; Brunvoll, J. *J. Organomet. Chem.* **1976**, *107*, 273.

(22) This value for manganocene (doublet) and cobaltocene is calculated as the difference between the experimental value and averaged calculated d(C−M) (M = Mn or Co), as the Cp rings are not calculated to be planar. The averaged value is 2.101 and 2.096 Å for the eclipsed and staggered conformers, respectively, for manganocene (doublet) and is 2.068 and 2.074 Å for the eclipsed and staggered conformers, respectively, for cobaltocene.

(23) Takasagawa, F.; Koetzle, T. F. *Acta Crystallogr.* **1979**, *B35*, 1074.

(24) Bérces, A.; Ziegler, T.; Fan, L. *J. Phys. Chem.* **1994**, *98*, 1584.

(25) (a) Fischer, E. O.; Leipfinger, H. *Z. Naturforsch., B: Anorg. Chem.* **1955**, *10*, 353. (b) Leipfinger, H. *Z. Naturforsch., B: Anorg. Chem.* **1959**, *13*, 53. (c) Voitlander, J.; Schimitschek, E. *Z. Elektrochem.* **1957**, *61*, 941. (d) Wilkinson, G.; Cotton, F. A.; Birmingham, J. M. *J. Inorg. Nucl. Chem.* **1956**, *2*, 95. (e) Konig, E.; Desai, V. P.; Kanellakopulos, B.; Klenze, R. *Chem. Phys.* **1980**, *54*, 109. (f) Hebandanz, N.; Kohler, F. H.; Muller, G.; Riede, J. *J. Am. Chem. Soc.* **1986**, *108*, 3281.

(26) Famiglietti, C.; Baerends, E. *J. Chem. Phys.* **1981**, *62*, 407.

(27) (a) Haaland, A. *Acc. Chem. Res.* **1979**, *12*, 415. (b) Coutiere, M.-M.; Demuynck, J.; Veillard, A. *Theor. Chim. Acta* **1982**, *27*, 281. (c) Rohmer, M.-M.; Veillard, A.; Wood, M. H. *Chem. Phys. Lett.* **1974**, *29*, 466. (d) Rohmer, M.-M.; Veillard, A. *Chem. Phys. Lett.* **1975**, *11*, 349. (e) Prins, R. *Mol. Phys.* **1970**, *19*, 603.

(28) (a) Evans, S.; Green, M. L. H.; Jewitt, B.; Orchard, A. F.; Pygall, C. F. *J. Chem. Soc., Faraday Trans. 2* **1972**, *68*, 1847. (b) Evans, S.; Green, M. L. H.; Jewitt, B.; King, G. H.; Orchard, A. F. *J. Chem. Soc., Faraday Trans. 2* **1974**, *70*, 356.

(29) (a) Aroney, M.; Le Fevre, R. J. W.; Sumasundaram, K. *J. Chem. Soc.* **1960**, 1812. (b) Le Fevre, R. J. W.; Murphy, D. S. N.; Saxby, J. D. *Aust. J. Chem.* **1971**, *14*, 1057.